Front. Environ. Sci. Eng. 2021, 15(1): 1
https://doi.org/10.1007/s11783-020-1293-2

RESEARCH ARTICLE

Evaluation of the technoeconomic feasibility of electrochemical hydrogen peroxide production for decentralized water treatment

Yang Li, Yixin Zhang, Guangshen Xia, Juhong Zhan, Gang Yu, Yujue Wang (✉)

School of Environment, State Key Joint Laboratory of Environmental Simulation and Pollution Control, Beijing Key Laboratory for Emerging Organic Contaminants Control, Tsinghua University, Beijing 100084, China

HIGHLIGHTS

- Gas diffusion electrode (GDE) is a suitable setup for practical water treatment.
- Electrochemical H_2O_2 production is an economically competitive technology.
- High current efficiency of H_2O_2 production was obtained with GDE at 5–400 mA/cm^2.
- GDE maintained high stability for H_2O_2 production for ~1000 h.
- Electro-generation of H_2O_2 enhances ibuprofen removal in an E-peroxone process.

GRAPHIC ABSTRACT

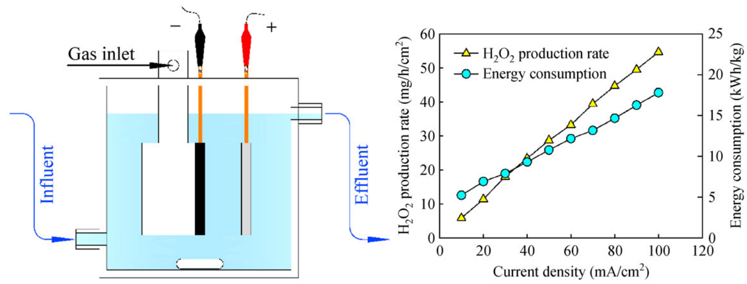

ABSTRACT

This study evaluated the feasibility of electrochemical hydrogen peroxide (H_2O_2) production with gas diffusion electrode (GDE) for decentralized water treatment. Carbon black-polytetrafluoroethylene GDEs were prepared and tested in a continuous flow electrochemical cell for H_2O_2 production from oxygen reduction. Results showed that because of the effective oxygen transfer in GDEs, the electrode maintained high apparent current efficiencies (ACEs,>80%) for H_2O_2 production over a wide current density range of 5–400 mA/cm^2, and H_2O_2 production rates as high as ~202 mg/h/cm^2 could be obtained. Long-term stability test showed that the GDE maintained high ACEs (>85%) and low energy consumption (< 10 kWh/kg H_2O_2) for H_2O_2 production for 42 d (~1000 h). However, the ACEs then decreased to ~70% in the following 4 days because water flooding of GDE pores considerably impeded oxygen transport at the late stage of the trial. Based on an electrode lifetime of 46 days, the overall cost for H_2O_2 production was estimated to be ~0.88 \$/kg H_2O_2, including an electricity cost of 0.61 \$/kg and an electrode capital cost of 0.27 \$/kg. With a 9 cm^2 GDE and 40 mA/cm^2 current density, ~2–4 mg/L of H_2O_2 could be produced on site for the electro-peroxone treatment of a 1.2 m^3/d groundwater flow, which considerably enhanced ibuprofen abatement compared with ozonation alone (~43%–59% vs. 7%). These findings suggest that electrochemical H_2O_2 production with GDEs holds great promise for the development of compact treatment technologies for decentralized water treatment at a household and community level.

ARTICLE INFO

Article history:
Received 21 April 2020
Revised 7 June 2020
Accepted 7 June 2020
Available online 9 July 2020

Keywords:
Advanced oxidation process
Electro-peroxone
Gas diffusion electrode
Hydrogen peroxide
Oxygen reduction

1 Introduction

Hydrogen peroxide (H_2O_2) is an indispensable chemical for a variety of advanced oxidation processes (AOPs) that are commonly used in water treatment, such as the Fenton (Fe^{2+}/H_2O_2), ultraviolet/H_2O_2 (UV/H_2O_2), and peroxone (O_3/H_2O_2) processes (Lu et al., 2018a; von Gunten, 2018; Yang et al., 2018; Zhang et al., 2019). Currently, H_2O_2 is produced almost exclusively by the anthraquinone process on an industrial scale (Campos-Martin et al., 2006; Zhou et al., 2019). The anthraquinone process is a large-scale centralized production process that requires massive infrastructure and significant energy input. To minimize transportation costs, the crude H_2O_2 obtained from the anthraquinone process is usually purified, concentrated, and then marketed as aqueous solutions with ~30 wt.%–70 wt.% H_2O_2. However, concentrated H_2O_2 is explosive

✉ Corresponding author
E-mail: wangyujue@tsinghua.edu.cn

and corrosive (Yang et al., 2018). The risks involved in the transport and storage of concentrated H_2O_2 stocks thus have considerably limited the application of H_2O_2-based AOPs in some cases, such as decentralized water treatment (Barazesh et al., 2015; von Gunten, 2018; Yang et al., 2018). Therefore, it is highly desired that H_2O_2 can be produced on site and on demand during water treatment in an energy-efficient, environmental friendly, and safe way.

Electrochemical H_2O_2 production from two-electron oxygen reduction reaction (ORR) has been considered a promising approach to produce H_2O_2 on site for water treatment (Wang et al., 2018b; Yang et al., 2018). The in situ production of H_2O_2 avoids the transport and storage of H_2O_2 stocks and can thus considerably enhance the safety and flexibility of H_2O_2-based AOPs. Over the past years, a variety of electricity-driven AOPs (EAOPs) have been developed based on the in situ generation of H_2O_2 from ORR, for example, the electro-Fenton (E-Fenton) (Brillas et al., 1996; Oturan et al., 1999), electro-peroxone (E-peroxone) (Yuan et al., 2013), and electrochemically driven UV/H_2O_2 (E-UV/H_2O_2) processes (Barazesh et al., 2015; Frangos et al., 2016). A great number of bench- and pilot-scale studies have demonstrated that these EAOPs can generally achieve similar or even better water treatment performance compared with their conventional counterparts (Brillas et al., 2009; Turkay et al., 2017b; Wang et al., 2018b). Therefore, it has been expected that these EAOPs will play an increasingly important role in future urban water systems if they can be successfully scaled up (von Gunten, 2018; Wang et al., 2018b; Yang et al., 2018).

While much progress has been made on electrochemical H_2O_2 production, its technoeconomic feasibility for practical water treatment has yet to be evaluated (Yang et al., 2018; Zhou et al., 2019). To be economically competitive, the cost of electrochemical H_2O_2 production must be competitive with that of the conventional way of H_2O_2 supplying (i.e., purchasing, transport, and storage of H_2O_2 stocks for water treatment). The cost of electrochemical H_2O_2 production includes mainly two parts, the energy consumption of electrolysis operation and the capital cost of electrodes (Yang et al., 2018). The reported energy consumption of H_2O_2 production vary significantly in literature, e.g., from ~3.1 to 60 kWh/kg H_2O_2 (Sheng et al., 2014; Yu et al., 2015; Lu et al., 2017; Pérez et al., 2019). Based on the electricity price of ~0.066 $/kWh (USEIA, 2016), these energy consumptions translate to ~0.20–4.0 $/kg H_2O_2. In comparison, the market price of H_2O_2 stock fluctuates between ~0.7 and 1.2 $/kg on 100 wt.% product basis (Ciriminna et al., 2016). Notably, while some studies have shown that H_2O_2 could be electrochemically produced at considerably lower electricity costs (e.g., 0.1–0.3 $/kg H_2O_2) than the market price of H_2O_2 stock (Barazesh et al., 2015), the current densities used in these studies (e.g., ~0.4–1.5 mA/cm^2) are probably too low for practical applications, where high current densities (several tens to hundreds of mA/cm^2) are desired to obtain high H_2O_2 production rate, minimize electrode surface (and capital cost), and construct compact electrochemical reactor (Wang et al., 2018b; Yang et al., 2018; Chaplin, 2019). This information suggests that the electricity cost of H_2O_2 production needs to be more relevantly evaluated under realistic operating conditions of water treatment. Moreover, to the best of our knowledge, the capital cost of electrode for H_2O_2 production has not been evaluated in previous studies.

More importantly, for decentralized water treatment, the electrode must be able to maintain high stability for H_2O_2 production over long-term operation and varying operating conditions (Zhou et al., 2019). Because of their low cost, high selectivity for two-electron ORR, and other favorable characteristics (e.g., chemical resistance and non-toxicity), carbonaceous materials are generally considered the most relevant catalysts for electrochemical H_2O_2 production in water treatment applications (Lu et al., 2018b). Various carbon-based electrodes have been developed for H_2O_2 electro-generation in EAOPs, for example, carbon felt, carbon black-polytetrafluoroethylene (CB-PTFE), activated carbon fiber, and reticulated vitreous carbon (Brillas et al., 2009; Turkay et al., 2017a; Wang et al., 2018b). These carbon-based electrodes generally exhibit good stability in short-term trials (e.g., laboratory-scale multi-cycle batch tests) (Sheng et al., 2014; Yu et al., 2015; Zhang et al., 2016). However, the time frame of the short-term trials is typically just several to several tens of hours, which are too short to draw convincing conclusions on the long-term stability of electrode. As the long-term stability of electrode is critical for maintaining robust water treatment performance and minimizing the capital cost of electrode, longer time trials are needed to evaluate this critical issue for practical applications.

The main objective of this study was to evaluate the technoeconomic feasibility of electrochemical H_2O_2 production for practical water treatment applications. A continuous electrochemical cell was developed to produce H_2O_2 under realistic operating conditions water treatment. The effects of electrode configurations and major process parameters (e.g., current density, interelectrode distance, flow rate, and conductivity) were investigated systematically. The stability of electrode for H_2O_2 production was evaluated in a long-term trial (~1100 h). Finally, the feasibility of electrochemical H_2O_2 production for micropollutant abatement in groundwater by the E-peroxone process was evaluated.

2 Materials and methods

2.1 Chemicals and water sample

Sodium sulfate, potassium titanium oxalate, anhydrous alcohol, and concentrated sulfuric acid were purchased from Beijing Chemical Works Co., China. H_2O_2 solutions (30 wt.%) were shipped from Sigma-Aldrich. Ibuprofen was purchased from Aladdin Reagent Co., Ltd. (Shanghai, China) and used as a model for ozone-resistant compound. Carbon black (CB) powder (Vulcan XC-72, Cabot Corp., USA) and polytetrafluoroethylene (PTFE) dispersion (60 wt.%) were purchased from Hesen electric Co. Ltd., Shanghai, China. A groundwater sample was collected in the north-west suburban of Beijing (see Table 1 for the water quality parameters).

Table 1 Water quality parameters of the groundwater used in this study

Parameters	Value
pH	7.57
DOC (mg/L)	1.60
HCO_3^- (mg/L)	302
CO_3^{2-} (mg/L)	–
Cl^- (mg/L)	30.5
SO_4^{2-} (mg/L)	56.6
Na^+ (mg/L)	21.1
Ca^{2+} (mg/L)	64.5
Mg^{2+} (mg/L)	30.2
Conductivity (μS/cm)	806

2.2 Electrode preparation

Carbon black-polytetrafluoroethylene (CB-PTFE) electrodes were prepared following the procedure described previously (Wang et al., 2012). Appropriate amounts of Vulcan XC-72 CB powder, PTFE dispersion, and anhydrous alcohol were mixed in an ultrasonic bath for 15 min. The mixture was then gently heated to evaporate alcohol at 80°C. The resulting CB-PTFE paste was compressed to form a sheet with a thickness of ~0.5 mm in a press. Next, two pieces of the CB-PTFE sheet, together with a nickel mesh in their middle as the current collector, were compressed at a pressure of 20 MPa for 5 min, followed by calcination at 350°C for 1 h to form the CB-PTFE electrode. Vulcan XC-72 was one of the most commonly used carbon materials for preparing CB-PTFE electrodes, whose properties have been well characterized in a number of previous studies (Assumpção et al., 2011; Valim et al., 2013; Stoerzinger et al., 2015).

For H_2O_2 electro-generation, the prepared CB-PTFE electrodes were either directly submerged in electrolytes aerated with an oxygen (O_2) gas (i.e., in the traditional submerged and aerated electrode (SAE) configuration, see Fig. 1(a)), or assembled with a gas chamber (3 cm × 3 cm × 2.4 cm) to form a gas diffusion electrode (GDE), which were then submerged in electrolytes to produce H_2O_2 using O_2 fed in the gas chamber as O_2 source for ORR (see Fig. 1(b)).

2.3 Electrochemical H_2O_2 production

Electrochemical H_2O_2 production experiments were conducted in a continuous flow electrochemical cell (8.8 cm × 8 cm × 10 cm) with a three-electrode system (see Fig. 1(c)). The cathode was the CB-PTFE electrode in the SAE or GDE configuration (exposed area of 3 cm × 3 cm). The anode was a platinum mesh (exposed area of 3 cm × 3 cm). During the experiments, the cathodic potentials were monitored using a saturated calomel electrode as the reference electrode. The selected groundwater was amended with 0.05–0.1 mol/L Na_2SO_4, then continuously fed into the bottom of the electrochemical cell and discharged at the top. The flow rate was regulated between 5 and 40 mL/min, which corresponds to a hydraulic residence time (HRT) of 80 and 10 min in the cell.

During electrochemical H_2O_2 production with the SAE cathode, a pure oxygen gas (99.9%) was continuously aerated in the electrochemical cell using a fine bubble diffuser at varying flow rates between 0.25 and 2.0 L/min. In contrast, no oxygen aeration was applied during electrochemical H_2O_2 production with the GDE cathode. Rather, the pure oxygen gas was passed through the gas chamber at a constant flow rate of 0.25 L/min, whereby oxygen in the gas chamber can diffuse in the micropores of CB-PTFE matrix to react with H^+ from the electrolyte and electron from the electrode to yield H_2O_2. During the experiments, the solution was vigorously agitated with a magnetic stirring bar to achieve homogeneous solution.

The apparent current efficiency, energy consumption, and electrode capital cost for H_2O_2 production are calculated using Eqs. (1), (2), and (3), respectively.

$$\eta = \frac{nF\int_0^t C_{H_2O_2} Q\mathrm{d}t}{3.6 \times 34S\int_0^t j\mathrm{d}t} \times 100\%, \tag{1}$$

$$EC = \frac{S\int_0^t jU\mathrm{d}t}{\int_0^t C_{H_2O_2} Q\mathrm{d}t} \times 10^{-3}, \tag{2}$$

$$C_{\mathrm{electrode}} = \frac{P_{\mathrm{electrode}} S}{\int_0^T C_{H_2O_2} Q\mathrm{d}t} \times 10^3, \tag{3}$$

where η is the apparent current efficiency for H_2O_2 electro-generation (%), n is the number of electrons consumed for converting 1 mol of O_2 to H_2O_2 (2 electrons), F is the Faraday constant (96485 C/mol), Q is the flow rate of water (m^3/h), $C_{H_2O_2}$ is the concentration of H_2O_2 (mg/L), S is the cathode area (cm^2), t is the electrolysis time (h), j is the cathodic current density (mA/cm^2), EC is the energy consumption of H_2O_2 production (kWh/kg), U is the cell

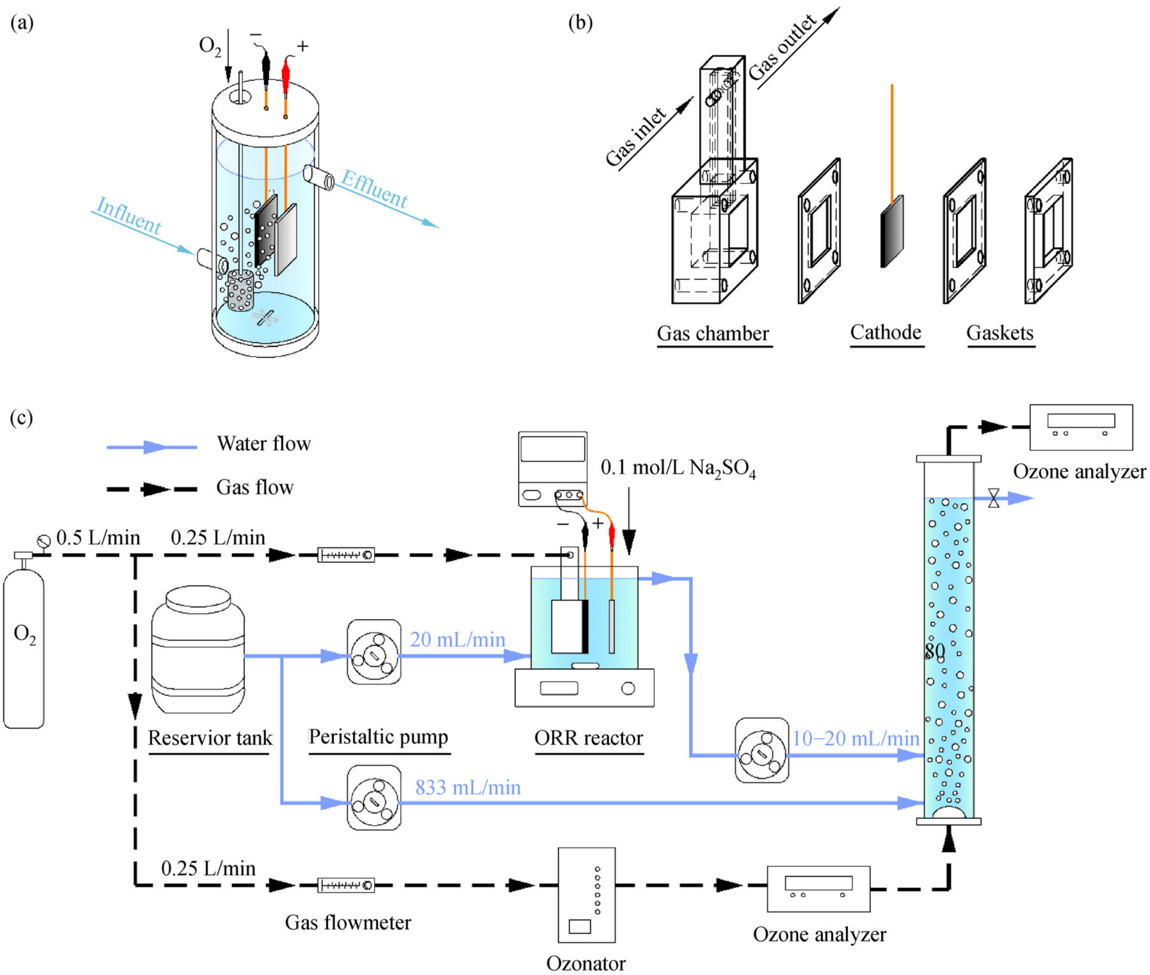

Fig. 1 Scheme of (a) electrochemical cell with the submerged and aerated electrode (SAE) and (b) the gas diffusion electrode (GDE), and (c) the electro-peroxone system for groundwater treatment.

voltage (V), $C_{electrode}$ is the electrode capital cost for H_2O_2 production ($/kg), $P_{electrode}$ is the cost per unit cathode area ($/cm^2), T is the lifetime of electrode (h).

2.4 Micropollutant abatement by ozonation and the E-peroxone process

To evaluate the effects of electrochemical H_2O_2 production on water treatment, a pilot scale E-peroxone system was developed by combining the electrochemical cell and an ozone system, then tested for micropollutant abatement in the selected groundwater (see Fig. 1(c) for the scheme of the system). The groundwater in the water tank was added with 100 µg/L ibuprofen (as a model compound for ozone-resistant micropollutant), then continuously fed into the bottom of the ozone column (10 cm i.d., 120 cm height, effective volume of 8.3 L) at a flow rate of 50 L/h (833 mL/min, corresponding to a HRT of 10 min in the column). Meanwhile, a side stream of the groundwater (20 mL/min, amended with 0.1 mol/L Na_2SO_4) was passed through the electrochemical cell for H_2O_2 production at a current density of 40 mA/cm^2 and HRT of 20 min. The electrochemical cell effluent was then continuously fed in the ozone reactor to mix with the mainstream groundwater. Simultaneously with the electro-generation of H_2O_2, an ozone-containing oxygen gas (O_3 = 18.7 mg/L) was produced by passing a pure oxygen gas (99.9%) through an ozone generator (OL80F/DST, Ozone services, Canada), and then continuously bubbled into the ozone column at a constant flow rate of 0.25 L/min. The E-peroxone treatment was operated with a HRT of 10 min. The treated groundwater was then discharged at the top of the ozone column.

2.5 Analytical methods

H_2O_2 concentration was measured using the potassium titanium (IV) oxalate method (Sellers, 1980). O_3 concentrations in the inlet gas and off gas of the ozone column were followed using ozone analyzers (BMT 964, Ozone

Systems Technology International Inc., Germany). Ibuprofen concentrations were measured with an ultraperformance liquid chromatography/tandem mass spectrometry (Agilent LC1290/QQQ6460, Agilent, USA) using the protocol described by (Yao et al., 2018).

3 Results and discussion

3.1 Comparison of SAE and GDE for H_2O_2 production

Figure 2(a) shows the evolution of H_2O_2 concentrations in the electrochemical cell effluent during electrolysis with the SAE cathode (HRT of 10 min). During the experiments, applied current densities were stepwise increased every 30 min to evaluate the effects of current density on H_2O_2 production. When a low current density of 5 mA/cm^2 was applied, H_2O_2 concentrations in the cell effluents were generally the same (~5 mg/L) regardless of the oxygen flow rates (0.25–2.0 L/min). However, as the current densities were stepwise increased, H_2O_2 concentrations exhibited different dynamics for the samples aerated with varying flow rates of oxygen. Specifically, when the current density was increased to 10 mA/cm^2, H_2O_2 concentrations increased similarly to ~9.5 mg/L for the samples aerated with 0.5–2.0 L/min O_2, but decreased abruptly to < 1 mg/L for the sample aerated with 0.25 L/min O_2. Similar abrupt drops in H_2O_2 concentrations and ACE for H_2O_2 production were also observed for the samples aerated with 0.5, 1.0, and 2.0 L/min O_2 as the current densities was stepwise increased to 15, 20, and 25 mA/cm^2, respectively (Figs. 2(a) and 2(b)).

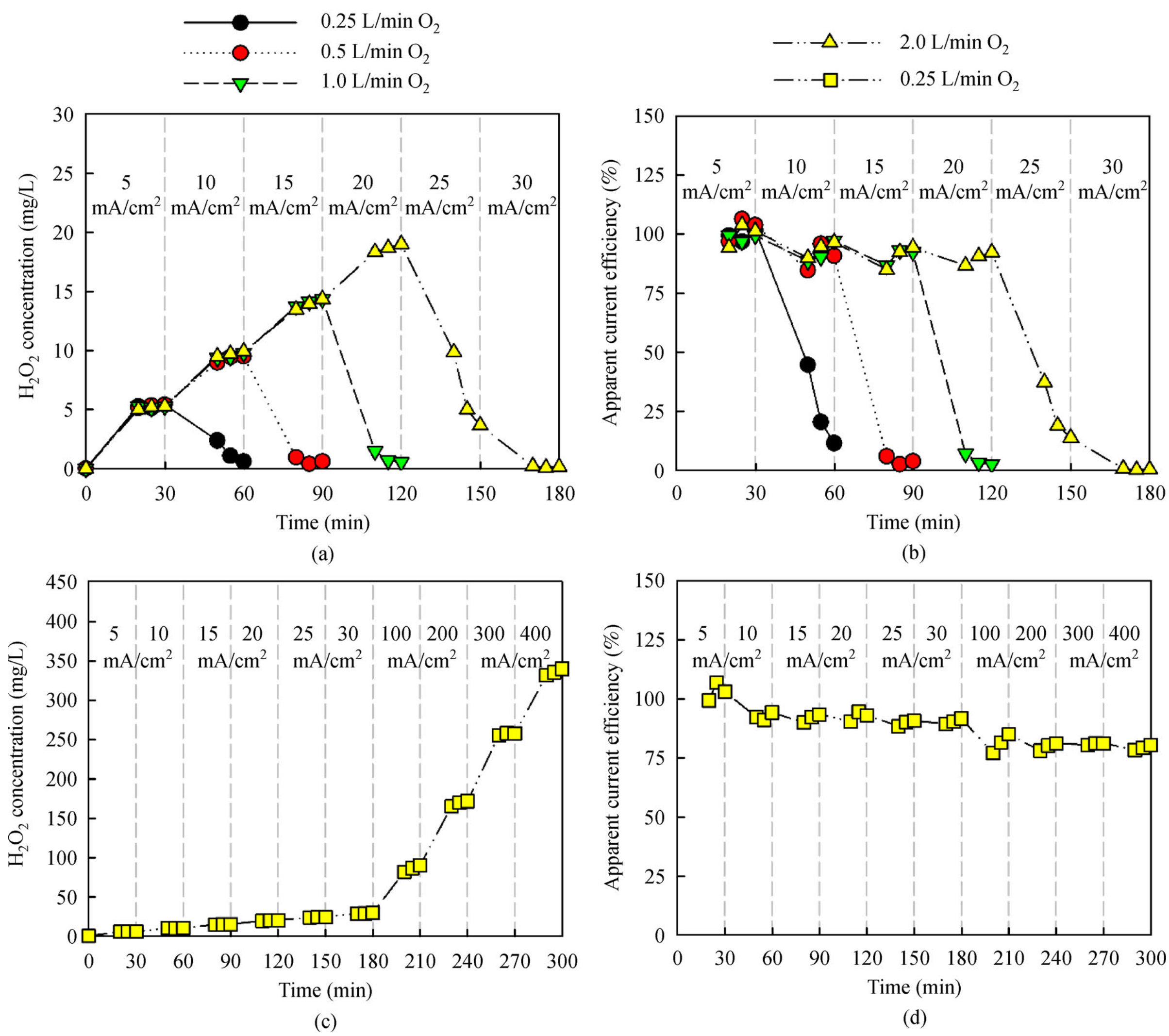

Fig. 2 Evolution of H_2O_2 concentrations and apparent current efficiency for H_2O_2 during electrolysis with the submerged and aerated electrode (a and b) and with gas diffusion electrode (c and d). Reaction conditions: HRT = 10 min, water flow rate = 40 mL/min, electrolyte = 0.1 mol/L Na_2SO_4, electrode area = 2 cm × 2 cm for the SAE and GDE, O_2 flow rates = 0.25–2 L/min for the SAE and 0.25 L/min for the GDE.

The results shown in Fig. 2(a) indicate that oxygen flow rates have a significant influence on electrochemical H_2O_2 production with the SAE cathodes. Due to oxygen aeration, numerous oxygen microbubbles are generated in the solution. Some oxygen microbubbles, together with dissolved oxygen (DO), can then diffuse to the cathode surface to supply O_2 for ORR to H_2O_2 (Tang et al., 2018; Zhou et al., 2019). The CB-PTFE electrodes used in this study have a high selectivity for two-electron ORR to H_2O_2 (Wang et al., 2015). When ORR at the cathode is limited by applied current densities rather than by O_2 mass transfer, high ACEs for H_2O_2 production (e.g., >90%) can generally be obtained with the CB-PTFE electrode (Wang et al., 2015). Figures 3(a) and 3(b) show that when a low current density of 5 mA/cm^2 was applied, similar H_2O_2 concentration (~5 mg/L) and high ACEs (generally >95%) were obtained irrespective of the flow rate of oxygen aeration. These observations suggest that ORR is current limited under the test conditions. However, as current densities are progressively increased, ORR to H_2O_2 may change from current limited to oxygen mass transfer limited (Xia et al., 2017). When there are insufficient quantities of O_2 in the cathodic diffusion layer to accepted electrons transferred at the cathode, side reactions such as further reduction of H_2O_2 to H_2O are promoted, which will result in significant decreases in H_2O_2 concentrations and ACEs for H_2O_2 production (Xia et al., 2017). Overall, the results shown above indicate that although increasing the flow rates of oxygen aeration can result in more oxygen microbubbles in the solution and thus enhance oxygen transfer to the cathode, this approach is not an effective way to supply O_2 to the SAE cathode. Therefore, electrochemical H_2O_2 production can only be stably operated at relatively low current densities ($\leqslant$20 mA/cm^2) with the SAE cathodes even when high flow rates of oxygen were aerated.

In contrast to the SAE electrode, H_2O_2 concentrations increased monotonically with increasing applied current densities up to 400 mA/cm^2 (the highest current density our DC power could supply) during electrolysis with the GDE cathode (Fig. 2(c)). In GDEs, oxygen in the gas chamber can diffuse in the porous CB-PTFE matrix, then react with H^+ and electron at a gas-electrode-liquid interface inside the electrode to yield H_2O_2, which then diffuses to the bulk electrolyte in the electrochemical cell (Zhou et al., 2019). The supply of O_2 through the porous structure and the formation of three-phase interface greatly enhance O_2 mass transfer and electron transfer between the multiple phases (Tang et al., 2018; Zhou et al., 2019). Therefore, significantly higher current densities can be applied during electrochemical H_2O_2 production with the GDE cathode without being subjected to O_2 mass transfer limitation.

Note that Fig. 2(d) shows that with increasing current densities from 5 to 400 mA/cm^2, the ACEs for H_2O_2 production decreased gradually from ~100% to ~78% during electrolysis with the GDE cathode. These decreases can be mainly attributed to the accelerated decomposition of cathodically generated H_2O_2 by anodic oxidation at higher H_2O_2 concentrations (see the effects of HRT on H_2O_2 production for further discussion) (Brillas et al., 2009; Xia et al., 2017).

For practical applications, the rate of H_2O_2 production (mass of H_2O_2 produced per unit time and per unit cathode surface area) must be able to meet the required H_2O_2 doses in water treatment (Eq. (4)). Meanwhile, as shown in Eq. (5), the rate of H_2O_2 production is directly proportional to current density and ACE for H_2O_2 production.

$$r = \frac{D_{H_2O_2} Q_W}{S} \times 10^3, \tag{4}$$

$$r = \frac{122400 j\eta}{nF}, \tag{5}$$

where r is the mass of H_2O_2 produced per unit time and per unit cathode area (mg/h/cm^2), $D_{H_2O_2}$ is the required H_2O_2 dose for water treatment (mg/L), Q_W is the flow rate of water that needs to be treated (m^3/h), S is the cathode area (cm^2), j is the current density (mA/cm^2), η is the apparent efficiency for H_2O_2 electro-generation (%).

The SAE configuration is prone to suffer from O_2 mass transfer limitation and can therefore be only stably operated at relatively low current densities even when a high flow rate of oxygen was aerated (e.g., $\leqslant$20 mA/cm^2 with 2.0 L/min oxygen aeration, see Fig. 2(a)). Therefore, the highest rate of H_2O_2 production obtained during electrolysis with the SAE cathode was only ~11.2 mg/h/cm^2 (see Fig. 3 inset). This means that large electrode surface area will be needed to produce required H_2O_2 doses when scaling up this process for decentralized water treatment applications (Eq. (4)). For example, based on the highest H_2O_2 production rate obtained during electrolysis with the SAE cathode, at least a ~0.9–9 m^2 cathode surface area is needed to produce 10 mg/L H_2O_2 in a 10–100 m^3/h water flow. The requirement of large electrode surface increases not only the capital cost of the electrodes (Eq. (3)), but also the difficulty in the construction of compact electrochemical reactor for practical applications.

In contrast, the GDEs allow H_2O_2 to be efficiently produced at significantly higher current densities (Figs. 2(c) and 2(d)), and H_2O_2 production rates as high as ~202 mg/h/cm^2 could be obtained during electrolysis with the GDE cathode (see Fig. 3). Consequently, a 0.05–0.5 m^2 GDE is sufficient to produce the required H_2O_2 dose (10 mg/L) in the aforementioned water flow (10–100 m^3/h). This result suggests that GDEs are a more feasible electrode configuration for the development of compact electrochemical reactors for practical water treatment applications.

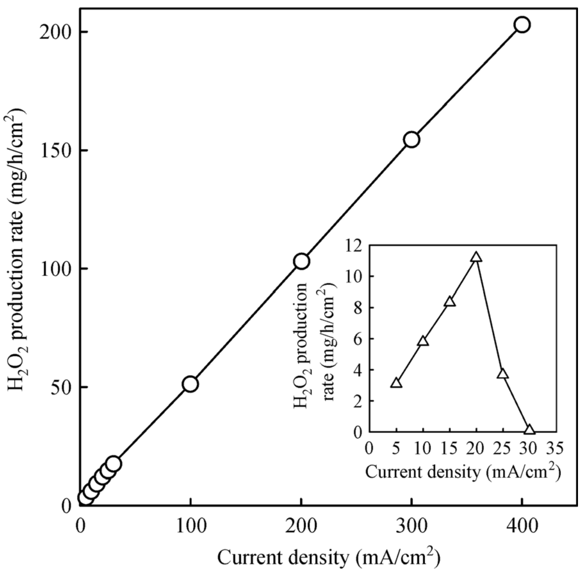

Fig. 3 H_2O_2 production rates as a function of applied current density during electrolysis with the GDE cathode and with the SAE cathode (inset). Reaction conditions: HRT = 10 min, water flow rate = 40 mL/min, electrolyte = 0.1 mol/L Na_2SO_4, electrode area = 2 cm × 2 cm for the SAE and GDE, O_2 flow rates = 0.25 L/min for the GDE and 2 L/min for the SAE.

3.2 Electrochemical H_2O_2 production with GDE

3.2.1 Effects of current density

Figure 4(a) shows that with increasing applied current densities from 10 to 100 mA/cm^2, H_2O_2 concentrations in the electrolytic cell effluent increased almost linearly during electrolysis with the GDE cathode. Adjusting current densities can thus offer a convenient and flexible way to control the H_2O_2 doses for water treatment. However, cell voltages increased concomitantly with increasing current densities (Fig. 4(b)). Consequently, the energy consumption for H_2O_2 production increased from 5.2 to 17.8 kWh/kg as the current densities were increased from 10 to 100 mA/cm^2 (Fig. 4(b)).

It is noted that the sales price of H_2O_2 stocks is ~0.7–1.2 \$/kg H_2O_2 (Ciriminna et al., 2016), which corresponds to ~10.6–18.2 kWh/kg H_2O_2 based on the electricity price of 0.066 \$/kWh (USEIA, 2016). Therefore, to be competitive with the market price of H_2O_2 stocks, the energy consumption of electrochemical of H_2O_2 production needs to be controlled below ~10–18 kWh/kg H_2O_2. Under the test conditions, this goal can be achieved by controlling the current densities lower than 50–100 mA/cm^2 (see Fig. 4(b)). Note that by optimizing operating conditions (e.g., reducing the interelectrode distance between the anode and cathode), higher current densities can be used without exceeding the target energy consumption (see discussion of Fig. 5).

Overall, the results presented above indicate that while higher current densities are desired to reduce the size and capital cost of electrodes and electrochemical cell, the electricity cost of H_2O_2 production increases with increasing current densities. Therefore, applied current densities need to be carefully controlled to balance the trade-off between capital cost and electricity cost of electrochemical H_2O_2 production.

3.2.2 Effects of interelectrode distance

By combining Eqs. (1) and (2), the energy consumption for H_2O_2 production can be expressed as:

$$EC = \frac{nFU}{122400\eta}. \tag{6}$$

According to this equation, the energy consumption for H_2O_2 production is directly proportional to the cell voltage

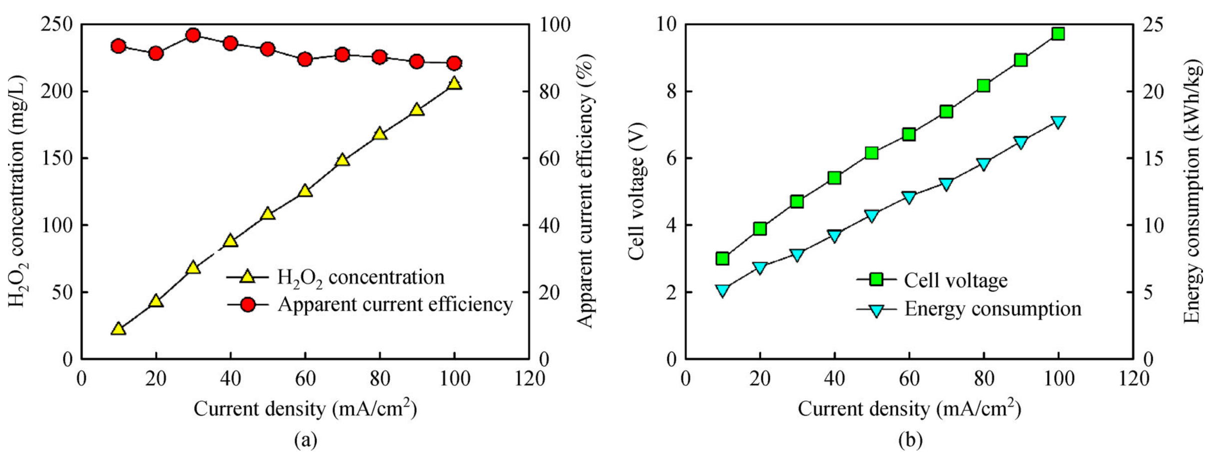

Fig. 4 (a) H_2O_2 concentrations and ACEs for H_2O_2 production, (b) cell voltage and energy consumption for H_2O_2 production as a function of applied current densities during electrochemical H_2O_2 production with the GDE cathode. Reaction conditions: HRT = 10 min, water flow rate = 40 mL/min, electrolyte = 0.1 M Na_2SO_4, electrode area = 3 cm × 3 cm, interelectrode distance = 2 cm.

and inversely proportional to the ACE for H_2O_2 production. As shown in Fig. 4(a), ACEs for H_2O_2 production changed insignificantly within the tested current density range of 10–100 mA/cm^2. This observation suggests that the increased energy consumption of H_2O_2 production at higher current densities is mainly caused by the increase of cell voltages (see Fig. 4(b)).

To get more information on the cell voltages, the potential profile in the electrochemical cell was measured using multimeters (Qiang et al., 2002) and is shown in Fig. 5(a). The cell voltage (the potential drop between the cathode and anode) is composed of three parts, the potential drops at the cathode- and anode-solution interface and the Ohmic drop in the solution. Note that because a reference electrode was placed between the anode and cathode to measure the cathodic potential, the anode and cathode had to be separated by a minimal interelectrode distance of ~1.5 cm, and most experiments were conducted with an interelectrode distance of 2 cm in this study. Due to the large interelectrode distance, the Ohmic drop in the solution (3.67 V) constituted a major fraction (~68.9%) of the cell voltage (5.33 V), whereas the potential drops at the anode- and cathode-solution interface constituted a minor fraction (23.6% and 7.5%, respectively). Because the electrolyte was homogeneous in the electrochemical cell, the Ohmic drop in the solution obeys the Ohm's Law and is directly proportional to the interelectrode distance. Figure 5(b) shows that as the interelectrode distance was decreased from 3 to 1.5 cm, cell voltages decreased almost linearly from ~6.82 to 4.93 V (R^2 = 0.998). By extrapolation, it is estimated that the cell voltage could be further reduced to ~3.65 V when an interelectrode distance of 0.5 cm is used, which will decrease the energy consumption for H_2O_2 production to 6.3 kWh/kg (compared with 9.5 kWh/kg with an interelectrode distance of 2 cm). This result indicates that minimizing the interelectrode distance is critical for energy-efficient H_2O_2 production when designing the electrochemical reactors for practical water treatment.

3.2.3 Effects of conductivity

To evaluate the effects of solution conductivity on electrochemical H_2O_2 production, the selected groundwater was amended with varying quantities of Na_2SO_4 (0.025–0.5 mol/L), then fed in the electrochemical cell for H_2O_2 production. Figure 6(a) shows that the ACEs for H_2O_2 production remained almost constant (~90%) when the conductivity was varied between 4.9 and 49.6 mS/cm. In contrast, cell voltages decreased considerably with increasing the solution conductivities (Fig. 6(a)), which in turn decreased the energy consumption of H_2O_2 production (Fig. 6(b)).

The results shown above indicate that solution conductivities have an important impact on the energy consumption of H_2O_2 production. To economically produce H_2O_2 at relatively high current densities, the solutions must have sufficiently high conductivities. For example, Fig. 6(b) shows that for a current density of 40 mA/cm^2, conductivities higher than 4.9–14.4 mS/cm are required to keep the energy consumption of H_2O_2 production lower than the sales price of H_2O_2 stocks (~10–18 kWh/kg). The conductivities of different water matrices vary significantly, e.g., ranging from typically < 1 mS/cm for most drinking water and municipal wastewater to > 50 mS/cm for some industrial wastewater, landfill leachate, and membrane concentrates (Wang et al., 2012; Barazesh et al., 2015; Wang et al., 2018a). The results shown herein

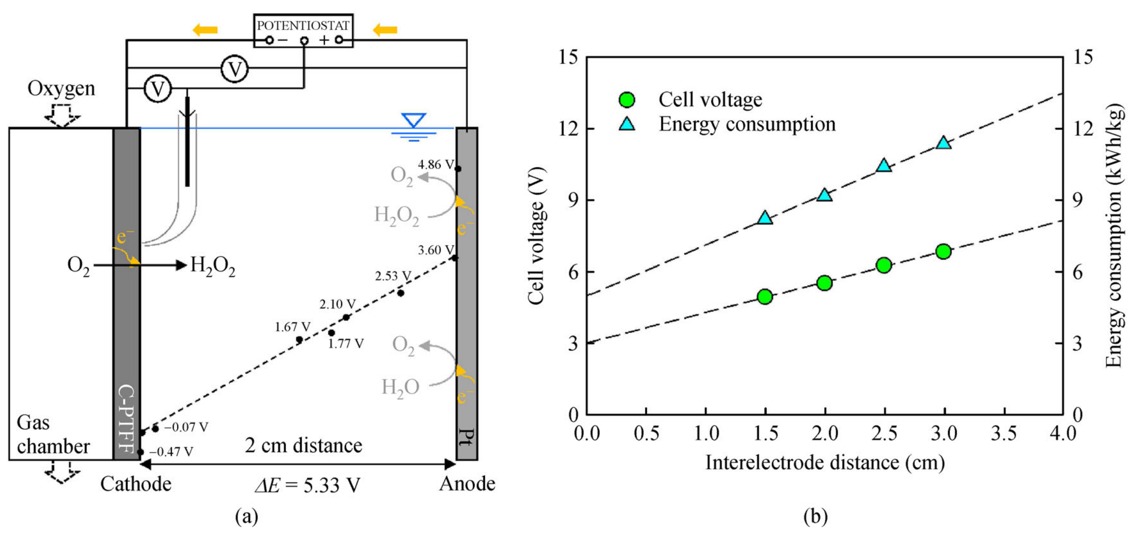

Fig. 5 (a) Potential profile in the electrochemical cell, (b) cell voltages and energy consumptions for H_2O_2 production as a function of interelectrode distance during electrochemical H_2O_2 production with the GDE cathode. Reaction conditions: HRT = 10 min, water flow rate = 40 mL/min, electrolyte = 0.1 mol/L Na_2SO_4, electrode area = 3 cm × 3 cm, current density = 40 mA/cm^2.

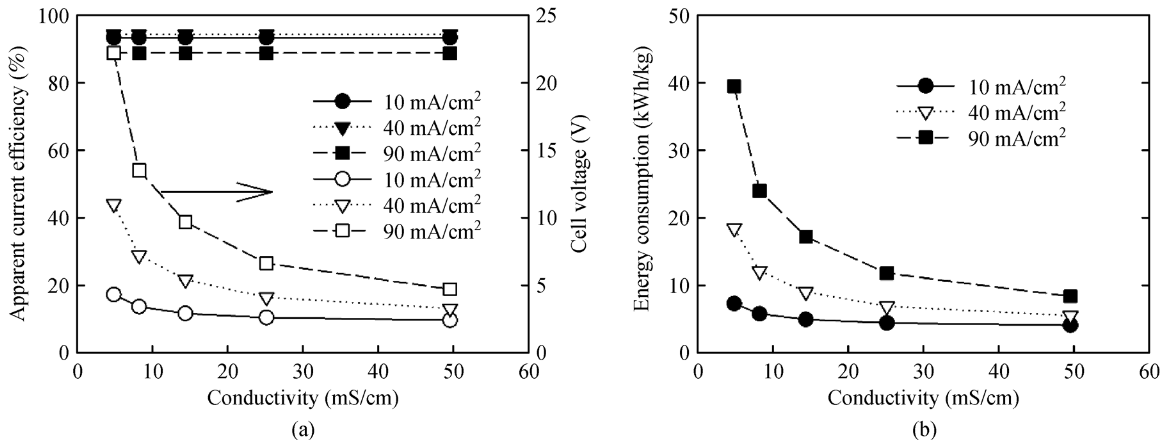

Fig. 6 Evolution of (a) apparent current densities and cell voltages, (b) energy consumption of H_2O_2 production as a function of solution conductivity during electrochemical H_2O_2 production with the GDE cathode. Reaction conditions: HRT = 10 min, water flow rate = 40 mL/min, electrolyte = 0.025–0.1 mol/L Na_2SO_4, electrode area = 3 cm × 3 cm, current density = 40 mA/cm^2

suggest that for water matrices that have high conductivities (e.g., >20 mS/cm), high current densities can be applied to produce H_2O_2 directly in the water to be treated. However, direct production of H_2O_2 in low-conductivity water matrices (e.g., drinking water and municipal wastewater) may not be economically feasible at the high current densities desired for practical applications (Barazesh et al., 2015; Wang et al., 2018a; Yao et al., 2018). A more feasible way is possibly to produce high-concentration H_2O_2 in electrolytes in a separate electrochemical cell, then feed the cell effluent to the water to be treated (see discussion below).

3.2.4 Effects of HRT

To evaluate the effects of HRT on electrochemical H_2O_2 production, the flow rate of the groundwater (amended with 0.1 mol/L Na_2SO_4) was varied between 5 and 40 mL/min, which results in a HRT of 10–80 min in the electrochemical cell. Figure 7(a) shows that as the HRTs were increased from 10 to 80 min, H_2O_2 concentrations in the effluent increased from ~94 to 349 mg/L. However, the ACEs for H_2O_2 production decreased considerably from ~98% to 46% with increasing the HRTs (Fig. 7(a)). Due to the significant decreases in ACEs (cell voltages did not change much with varying HRTs), the energy consumption for H_2O_2 production increased from ~8.6 to 17.4 kWh/kg as the HRTs were increased from 5 to 80 min (Fig. 7(b)).

The above results indicate that HRT has complex implications on the performance of electrochemical H_2O_2 production. On the one hand, increasing HRTs can result in higher H_2O_2 concentrations in the electrochemical cell effluent (Fig. 7(a)). Thus, smaller volumes of the cell effluent will be needed to supply the required H_2O_2 doses for subsequent water treatment. This is helpful to reduce the salt consumption for preparing the electrolyte solutions and the residual salt concentrations in the final effluent after water treatment. On the other hand, as H_2O_2

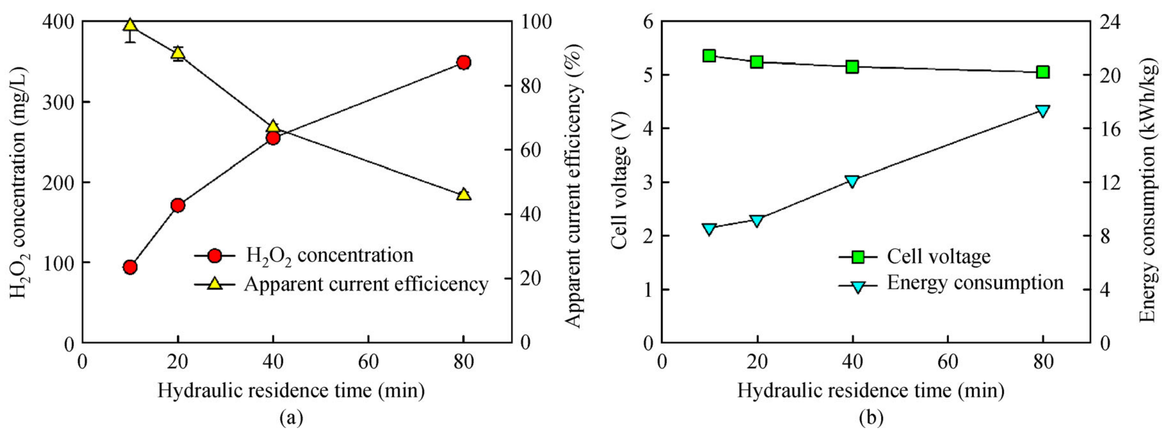

Fig. 7 Evolution of (a) H_2O_2 concentrations and ACEs for H_2O_2 production, (b) cell voltages and energy consumption for H_2O_2 production as a function of HRT during electrochemical H_2O_2 production with the GDE cathode. Reaction conditions: water flow rate = 5–40 mL/min, electrolyte = 0.1 mol/L Na_2SO_4, electrode area = 3 cm × 3 cm, current density = 40 mA/cm^2.

concentrations increase in the electrochemical cell, side reactions such as H_2O_2 decomposition by anodic oxidation are enhanced (Xia et al., 2017), which results in a decrease in the ACEs and an increase in the energy consumption of H_2O_2 production (Fig. 7(b)). By installing proton-exchange membrane to separate the cathodic and anodic compartment, the destruction of cathodically generated H_2O_2 by anodic oxidation can be prevented. Nevertheless, this approach increases the complexity and cost of electrochemical cell, and therefore is not employed in the present study. Overall, the results shown in Fig. 7 suggest that for practical applications, HRT needs to be optimized to balance the trade-off among the different factors and thus achieve better overall performance of water treatment.

3.2.5 Stability of electrode

To evaluate the stability of GDE cathodes, a new GDE cathode was made and then tested for continuous electrochemical H_2O_2 production for 46 days (~1100 h). Figure 8(a) shows that H_2O_2 concentrations in the effluent decreased gradually from ~186 to 166 mg/L during the first 42 d (~1000 h). However, they then exhibited a quick decrease during the last 4 d. Meanwhile, it was observed that some water had penetrated the CB-PTFE electrode to the gas chamber on the 46th d. Hence, the experiment was stopped thereafter. Despite some fluctuations, cell voltages showed a general slow increasing trend from initially ~5 to finally 5.5 V during the 46 d trial (Fig. 8(b)). Due to the changes in the ACEs for H_2O_2 production and cell voltages, the energy consumption of H_2O_2 production increased gradually from ~8.3 to 9.8 kWh/kg during the first 42 d, then increased quickly to 12.6 kWh/kg during the last 4 days (Fig. 8(b)).

The results shown in Fig. 8 demonstrate that in the long run, the performance of the GDE cathode for H_2O_2 production deteriorates. This deterioration can be possibly attributed to several events that occur gradually during electrochemical H_2O_2 production. A few studies have indicated that upon H_2O_2 exposure and/or negative polarization, some active sites of two-electron ORR on the carbon surface (e.g., pyridinic-N groups) will be gradually transformed to inactive or less active sites (e.g., pyrodonic-N) (Wang et al., 2019; Xia et al., 2020). Moreover, due to the high cathodic pH and migration of calcium ions in the groundwater, calcium carbonate ($CaCO_3$) precipitations formed gradually on the surface and inside the porous structure of the CB-PTFE cathode during the long-term trial (see SI Fig. S1). The $CaCO_3$ scaling may block some active sites of ORR on the electrode and thus lead to gradually declined efficiencies of the electrode for H_2O_2 production. Furthermore, due to the formation of $CaCO_3$ precipitations in the porous CB-PTFE structure, the hydrophobicity of the GDE decreases (Warsinger et al., 2015; Rezaei et al., 2018), which facilitates water seepage into the pores of the electrode under cathodic polarization conditions (Sheng et al., 2014) and eventually led to water penetration to the gas chamber on the 46th day. The flooding of pores in the CB-PTFE structure considerably impedes oxygen transport in the GDE cathode, thus leading to the quick decrease of H_2O_2 production at the late stage of the long-term trial (Fig. 8(a)).

Despite the gradual deterioration, the GDE cathode maintained a good performance for H_2O_2 production (ACEs $\geqslant$ 85%, energy consumption $\leqslant$ 10 kWh/kg) for 42 d (~1000 h) (Fig. 7). Based on the costs of raw materials (carbon black, PTFE dispersion, and nickel mesh) used to make the CB-PTFE electrode, the cost per unit electrode area is calculated to be ~0.0067 \$/cm^2 (see SI for the calculation detail). With a total production of ~0.225 kg H_2O_2 over the electrode lifetime, the capital cost of the electrode for H_2O_2 production is thus estimated to be ~0.27 \$/kg H_2O_2 (Eq. (3)). Meanwhile, the average energy consumption for H_2O_2 production is ~9.3 kWh/kg (equivalent to 0.61 \$/kg) during the 46 d trial. Therefore,

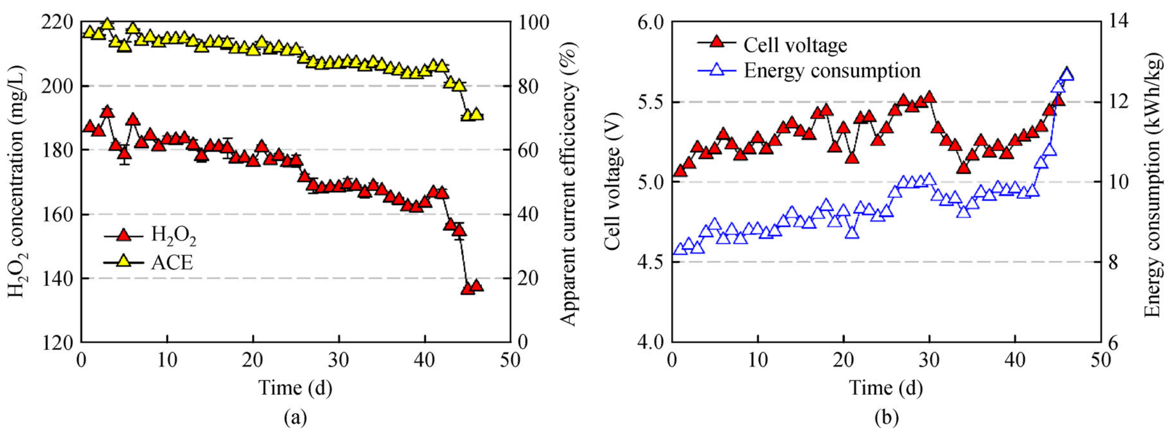

Fig. 8 Evolution of (a) H_2O_2 concentrations and ACEs for H_2O_2 production, (b) cell voltages and energy consumptions for H_2O_2 production during electrochemical H_2O_2 production with the GDE cathode. Reaction conditions: HRT = 20 min, water flow rate = 20 mL/min, electrolyte = 0.1 mol/L Na_2SO_4, electrode area = 3 cm × 3 cm, interelectrode distance = 2 cm, current density = 40 mA/cm^2

the overall cost of H_2O_2 production is estimated to be about 0.88 \$/kg H_2O_2 under the tested conditions. These data suggest that besides avoiding the risks linked to H_2O_2 transport and storage, electrochemical H_2O_2 production can be an economically competitive alternative to the conventional way of H_2O_2 supplying (0.7–1.2 \$/kg (Ciriminna et al., 2016)). In addition, the results also suggests that the capital cost of electrode can constitute a non-negligible fraction (~30% herein) of the overall cost for H_2O_2 production and thus should be taken into account when evaluating the economic feasibility of electrochemical H_2O_2 production for practical applications.

3.3 Electrochemical H_2O_2 production for water treatment

To evaluate the feasibility of electrochemical H_2O_2 production in the context of decentralized water treatment, the electrochemical cell was combined with a pilot ozonation system for micropollutant abatement in the selected groundwater (see Fig. 1(c) for the scheme). Due to its low background conductivity (Table 1), directly producing H_2O_2 in the selected groundwater is uneconomical at high current densities required for practical applications (see discussion in Section 3.1). Moreover, adding salts (e.g., Na_2SO_4 or NaCl) to raise the conductivity of the whole water flow that needs to be treated is also impractical because this approach consumes large amounts of salts and results in high concentrations of residual salts in the treated water. Therefore, a side stream of the groundwater (20 mL/min) was amended with 0.1 M Na_2SO_4, then passed through the electrochemical cell for H_2O_2 production. With a current density of 40 mA/cm^2 and HRT of 20 min, the electrochemical cell produced ~166 mg/L H_2O_2 in its effluent (Fig. 8(a)). A varying fraction of the cell effluent (10–20 mL/min) was then fed to the ozone column to mix with the mainstream groundwater (833 mL/min), followed by ozonation treatment (HRT = 10 min). With the dilution factor of ~42.7–84.3, the H_2O_2 doses were about 2.0–3.9 mg/L in the ozone column, and the residual Na_2SO_4 concentrations were ~168.4–332.6 mg/L in the ozonation effluent. In comparison, the suggested taste threshold of Na_2SO_4 in drinking water is 250 mg/L (WHO, 2011). These data indicate that for practical applications, high dilution factors are desired to minimize the residual salt concentrations in treated water. Otherwise, an additional desalination process will be needed to reduce the salt concentrations to below the regulated concentrations (Lin et al., 2020), resulting in an increase in the overall treatment process.

Figure 9(a) shows that when no electrochemical cell effluent was fed in the ozone column, ozonation alone abated only ~7% of ibuprofen spiked in the selected groundwater. In contrast, the abatement efficiency of ibuprofen was considerably increased to ~43%–59% when 10–20 mL/min of the cell effluent was fed in the ozone column. The low abatement efficiency of ibuprofen by ozonation alone can be mainly attributed to the low reactivity of ibuprofen with ozone (k_{O3} = 9.6 $M^{-1}\cdot s^{-1}$ (Huber et al., 2003)). Moreover, as shown in SI Fig. S2, while ~3.8 mg/L O_3 was transferred from the bubbled O_3/O_2 gas to the groundwater during ozonation alone, only ~0.8 mg/L O_3 decomposed in the ozone column (i.e., 3.0 mg/L of the transferred O_3 dose remained in the ozone column effluent). This observation indicates that the selected groundwater had a high ozone stability, which results in natural O_3 decomposition to hydroxyl radicals (•OH) a slow process in the groundwater (Wang et al., 2018a; Yao et al., 2018). Consequently, ibuprofen abate-

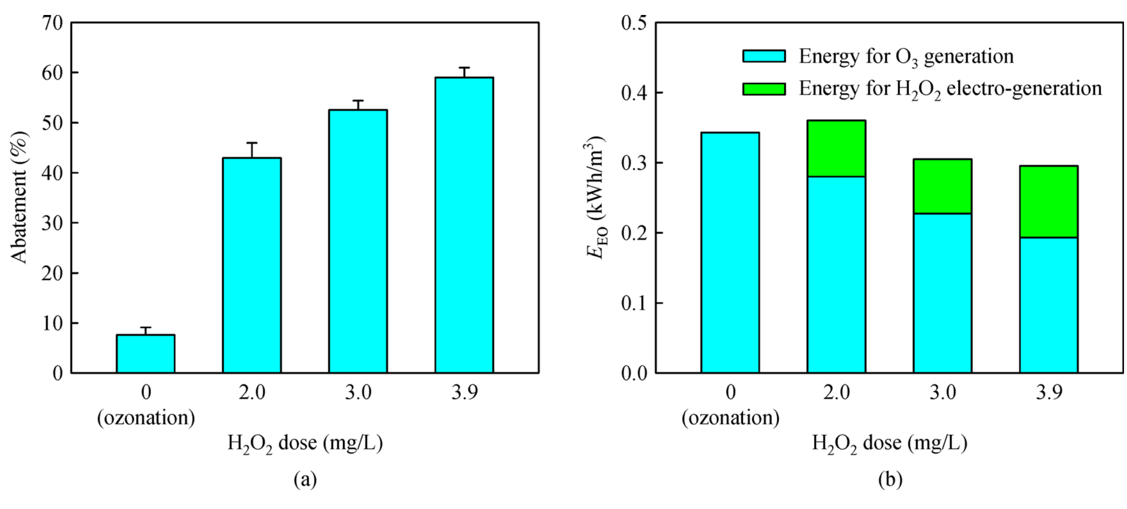

Fig. 9 (a) Ibuprofen abatement efficiency, (b) E_{EO} of ibuprofen abatement as a function of H_2O_2 doses during ozonation and the E-peroxone treatment of the selected groundwater. Operating conditions of electrochemical cell: HRT = 20 min, water flow rate = 20 mL/min, electrolyte = 0.1 mol/L Na_2SO_4, electrode area = 3 cm × 3 cm, interelectrode distance = 2 cm, current density = 40 mA/cm^2. Operating conditions of ozone column: HRT = 10 min, water flow rate = 833 mL/min, flow rate of electrochemical cell effluent = 10–20 mL/min, O_3/O_2 gas flow rate = 0.25 L/min, gas phase O_3 concentration = 18.7 mg/L.

ment by •OH oxidation is insignificant during ozonation alone.

In comparison, the combination of electrochemical H_2O_2 production with ozonation (i.e., the E-peroxone process) considerably enhanced ibuprofen abatement (Fig. 9(a)). These enhancements can be mainly attributed to the accelerated O_3 transfer and transformation to •OH by electro-generated H_2O_2 (Wang et al., 2018b; Yao et al., 2018). As shown in SI Fig. S2, under the same O_3-containing gas bubbling conditions, the transferred ozone doses increased from ~3.8 mg/L during ozonation alone to ~5.0–5.2 mg/L during the E-peroxone process fed with 10–20 mL/min electrolyzer effluent. In addition, the decomposed O_3 doses increased significantly from ~0.8 mg/L O_3 during ozonation to 4.6–5.0 mg/L O_3 during the E-peroxone process. These observations indicate that the feeding of H_2O_2-containing electrochemical cell effluent significantly accelerates O_3 transfer and decomposition in the ozone column. Besides accelerating O_3 decomposition to •OH, the •OH yield (moles of •OH formed per mole of O_3 consumed) from the reaction of O_3 with H_2O_2 (~50%) is also generally higher than those from natural O_3 decomposition in water matrix (~10%–30%) (von Sonntag and von Gunten, 2012; Wang et al., 2018a). Due to the H_2O_2-enhanced O_3 transformation to •OH, the E-peroxone process can considerably enhance ozone-resistant micropollutant abatement by •OH oxidation compared with ozonation alone (Wang et al., 2018b).

Based on the decomposed O_3 doses (i.e., ozone doses actually consumed in the zone column) and energy consumption for H_2O_2 production, the electrical energy demand to abate ibuprofen concentration by 1 order in 1 m^3 of water (E_{EO} (Bolton et al., 2001)) is calculated and shown in Fig. 9(b) (see SI for the calculation detail). Despite the extra energy consumption for H_2O_2 production, the E_{EO} values of the E-peroxone process (0.294–0.360 kWh/m^3) is generally comparable or slightly lower than that of ozonation alone (0.343 kWh/m^3). This finding indicates that the energy consumption for H_2O_2 production can be adequately compensated by the higher efficiency of the E-peroxone process for micropollutant abatement (Wang et al., 2018b; Yao et al., 2018).

The above results show that with a 9 cm^2 GDE cathode, typical H_2O_2 doses applied in H_2O_2-based AOPs (~3 mg/L (Barazesh et al., 2015)) can be produced on site for the treatment of 1–2 m^3/d water flow, which is sufficient for the daily use at a household level. In addition, due to the accelerated O_3 transfer and decomposition by electro-generated H_2O_2 (SI Fig. S2), significantly smaller ozone contactors can be used during water treatment by the E-peroxone process than by conventional ozonation (Yao et al., 2018). These findings suggest that electrochemical H_2O_2 production holds great promise for the development of compact treatment technologies for decentralized water treatment systems at a household and community level or even larger scale applications (Barazesh et al., 2015; von Gunten, 2018; Wang et al., 2018b).

Besides the E-peroxone process, electrochemical H_2O_2 production has been used to drive other EAOPs such as the E-Fenton, photoelectro-Fenton, and E-UV/H_2O_2 processes for water and wastewater treatment (Brillas et al., 2009; Barazesh et al., 2015; Frangos et al., 2016). Recently, there are an increasing number of pilot-scale studies that have evaluated the feasibility of these EAOPs for small-scale water and wastewater treatment (Plakas et al., 2016; Salmerón et al., 2018; Yao et al., 2018; Alcaide et al., 2020). The promising results shown in these studies suggest that because of their own characteristics, the various H_2O_2-based EAOPs may fit well into different niches in the future water treatment systems. For example, the E-Fenton process may provide a particularly suitable way to treat acid wastewater because of its high energy efficiency of •OH generation at low pH. In contrast, the E-peroxone process is more suitable to treat waters with circumneutral and basic pH due to the faster reaction of O_3 with H_2O_2 at elevated pH. Therefore, these H_2O_2-based EAOPs may together constitute an important component of next generation technologies for decentralized water treatment systems.

3.4 Implications

It is noted that the electrode materials and operating conditions employed in this study are far from being ideal. The catalyst, Vulcan XC72 carbon black, has a high selectivity but low activity for two-electron ORR to H_2O_2 (Assumpção et al., 2011; Yang et al., 2018). Many studies have shown that by tailoring with metals, metal oxides, and other materials, the activity of Vulcan XC72 for ORR can be considerably enhanced, thus reducing the cathodic overpotential during electrochemical H_2O_2 production (Valim et al., 2013; Stoerzinger et al., 2015; Paz et al., 2018). In addition, anodes with higher oxygen evolution activity can be used to decrease the overpotential of anode (Chen et al., 2017). Furthermore, by minimizing the interelectrode distance, the Ohmic drop in the solutions can also be substantially reduced (see Fig. 5(b)) (Pérez et al., 2019). This information indicates that there is still large room for the improvement of the system to reduce the cell voltages and thus energy consumption of H_2O_2 production.

The lifetime of the prepared GDE cathode (~46 d) still needs to be considerably extended to ensure stable long-term operations and to reduce the capital and maintenance cost for electrode replacement. To this end, several measures may be taken, for example, enhanced hydrophobic treatment of the electrode and periodic polarity reversal operation to mitigate $CaCO_3$ scaling and retard water penetration. Additional studies will be conducted to evaluate these measures and to further enhance the economic competitiveness of this technology for practical water treatment.

In addition, the results of this study demonstrate that the events that cause electrode deterioration (e.g., calcium carbonate precipitation and water penetration) occur only gradually during electrochemical H_2O_2 production. Therefore, the deterioration of electrode performance is a slow process, especially in the first several days (Fig. 8). The commonly used short-term stability tests that are conducted within a typical time frame of several to several tens of hours are unlikely to perceive such slow changes in the electrode performance (Sheng et al., 2014; Yu et al., 2015). More studies are needed to evaluate the electrode lifetime, the mechanisms and control strategies of electrode deterioration over longer time periods and realistic operating conditions for water treatment.

4 Conclusions

This study confirms the technoeconomic feasibility of electrochemical H_2O_2 production for practical water treatment. Because of the effective oxygen transfer in the GDE, high current densities (several tens to hundreds of mA/cm^2) can be applied to efficiently produce H_2O_2 with apparent current efficiencies generally >85% during electrolysis with the GDE cathodes. This allows compact electrochemical reactors to be developed for practical applications such as decentralized water treatment at a household and community level. The overall cost of electrochemical H_2O_2, including the electrode capital cost and electricity cost, was estimated to be ~0.88 $/kg under the test conditions and can be further decreased by optimizing the electrodes, electrochemical cell, and operating conditions. By combining H_2O_2 electro-generation with ozonation, the E-peroxone process considerably accelerated water treatment process and enhanced ozone-resistant micropollutant abatement compared with ozonation alone. These results indicate that electrochemical H_2O_2 production holds great promise for the development of compact treatment technologies for future urban water systems.

Acknowledgements This study is funded by the National Natural Science Foundation of China (Grant No. 51878370), the National Special Program of Water Pollution Control and Management (No. 2017ZX07202), and the special fund of State Key Joint Laboratory of Environment Simulation and Pollution Control (No. 18L01ESPC).

Electronic Supplementary material Supplementary material is available in the online version of this article at https://doi.org/10.1007/s11783-020-1293-2 and is accessible for authorized users.

References

Alcaide F, Álvarez G, Guelfi D R V, Brillas E, Sirés I (2020). A stable CoSP/MWCNTs air-diffusion cathode for the photoelectro-Fenton degradation of organic pollutants at pre-pilot scale. Chemical Engineering Journal, 379: 122417

Assumpção M H M T, De Souza R F B, Rascio D C, Silva J C M, Calegaro M L, Gaubeur I, Paixao T R L C, Hammer P, Lanza M R V, Santos M C (2011). A comparative study of the electrogeneration of hydrogen peroxide using Vulcan and Printex carbon supports. Carbon, 49(8): 2842–2851

Barazesh J M, Hennebel T, Jasper J T, Sedlak D L (2015). Modular advanced oxidation process enabled by cathodic hydrogen peroxide production. Environmental Science & Technology, 49(12): 7391–7399

Bolton J R, Bircher K G, Tumas W, Tolman C A (2001). Figures-of-merit for the technical development and application of advanced oxidation technologies for both electric- and solar-driven systems-(IUPAC Technical Report). Pure and Applied Chemistry, 73(4): 627–637

Brillas E, Mur E, Casado J (1996). Iron(II) catalysis of the mineralization of aniline using a carbon-PTFE O-2-fed cathode. Journal of the Electrochemical Society, 143(3): L49–L53

Brillas E, Sires I, Oturan M A (2009). Electro-Fenton process and related electrochemical technologies based on Fenton's reaction chemistry. Chemical Reviews, 109(12): 6570–6631

Campos-Martin J M, Blanco-Brieva G, Fierro J L (2006). Hydrogen peroxide synthesis: an outlook beyond the anthraquinone process. Angewandte Chemie International Edition in English, 45(42): 6962–6984

Chaplin B P (2019). The prospect of electrochemical technologies advancing worldwide water treatment. Accounts of Chemical Research, 52(3): 596–604

Chen Z, Chen S, Siahrostami S, Chakthranont P, Hahn C, Nordlund D, Dimosthenis S, Nørskov J K, Bao Z, Jaramillo T F (2017). Development of a reactor with carbon catalysts for modular-scale, low-cost electrochemical generation of H_2O_2. Reaction Chemistry & Engineering, 2(2): 239–245

Ciriminna R, Albanese L, Meneguzzo F, Pagliaro M (2016). Hydrogen peroxide: A Key chemical for today's sustainable development. ChemSusChem, 9(24): 3374–3381

Frangos P, Shen W H, Wang H J, Li X, Yu G, Deng S B, Huang J, Wang B, Wang Y J (2016). Improvement of the degradation of pesticide deethylatrazine by combining UV photolysis with electrochemical generation of hydrogen peroxide. Chemical Engineering Journal, 291: 215–224

Huber M M, Canonica S, Park G Y, Von Gunten U (2003). Oxidation of pharmaceuticals during ozonation and advanced oxidation processes. Environmental Science & Technology, 37(5): 1016–1024

Lin S, Lu Y, Ye B, Zeng C, Liu G, Li J, Luo H, Zhang R (2020). Pesticide wastewater treatment using the combination of the microbial electrolysis desalination and chemical-production cell and Fenton process. Frontiers of Environmental Science & Engineering, 14(1): 12

Lu S, Wang N, Wang C (2018a). Oxidation and biotoxicity assessment of microcystin-LR using different AOPs based on UV, O_3 and H_2O_2. Frontiers of Environmental Science & Engineering, 12(3): 12

Lu Y B, Liu G L, Luo H P, Zhang R D (2017). Efficient in-situ production of hydrogen peroxide using a novel stacked electrosynthesis reactor. Electrochimica Acta, 248: 29–36

Lu Z, Chen G, Siahrostami S, Chen Z, Liu K, Xie J, Liao L, Wu T, Lin D, Liu Y, Jaramillo T F, Nørskov J K, Cui Y (2018b). High-efficiency oxygen reduction to hydrogen peroxide catalysed by oxidized carbon materials. Nature Catalysis, 1(2): 156–162

Oturan M A, Aaron J J, Oturan N, Pinson J (1999). Degradation of chlorophenoxyacid herbicides in aqueous media, using a novel electrochemical method. Pesticide Science, 55(5): 558–562

Paz E C, Aveiro L R, Pinheiro V S, Souza F M, Lima V B, Silva F L, Hammer P, Lanza M R V, Santos M C (2018). Evaluation of H_2O_2 electrogeneration and decolorization of Orange II azo dye using tungsten oxide nanoparticle-modified carbon. Applied Catalysis B: Environmental, 232: 436–445

Pérez J F, Llanos J, Sáez C, López C, Cañizares P, Rodrigo M A (2019). Towards the scale up of a pressurized-jet microfluidic flow-through reactor for cost-effective electro-generation of H_2O_2. Journal of Cleaner Production, 211: 1259–1267

Plakas K V, Sklari S D, Yiankakis D A, Sideropoulos G T, Zaspalis V T, Karabelas A J (2016). Removal of organic micropollutants from drinking water by a novel electro-Fenton filter: Pilot-scale studies. Water Research, 91: 183–194

Qiang Z, Chang J H, Huang C P (2002). Electrochemical generation of hydrogen peroxide from dissolved oxygen in acidic solutions. Water Research, 36(1): 85–94

Rezaei M, Warsinger D M, Lienhard V J H, Duke M C, Matsuura T, Samhaber W M (2018). Wetting phenomena in membrane distillation: Mechanisms, reversal, and prevention. Water Research, 139: 329–352

Salmerón I, Plakas K V, Sirés I, Oller I, Maldonado M I, Karabelas A J, Malato S (2018). Optimization of electrocatalytic H_2O_2 production at pilot plant scale for solar-assisted water treatment. Applied Catalysis B: Environmental, 242: 327–336

Sellers R M (1980). Spectrophotometric determination of hydrogen peroxide using potassium titanium(IV) oxalate. Analyst (London), 105(1255): 950–954

Sheng Y P, Zhao Y, Wang X L, Wang R, Tang T (2014). Electrogeneration of H_2O_2 on a composite acetylene black-PTFE cathode consisting of a sheet active core and a dampproof coating. Electrochimica Acta, 133: 414–421

Stoerzinger K A, Risch M, Han B H, Shao-Horn Y (2015). Recent insights into manganese oxides in catalyzing oxygen reduction kinetics. ACS Catalysis, 5(10): 6021–6031

Tang C, Wang H F, Zhang Q (2018). Multiscale principles to boost reactivity in gas-involving energy electrocatalysis. Accounts of Chemical Research, 51(4): 881–889

Turkay O, Barisci S, Ozturk B, Ozturk H, Dimoglo A (2017a). Electro-peroxone treatment of phenol: process comparison, the effect of operational parameters and degradation mechanism. Journal of the Electrochemical Society, 164(9): E180–E186

Turkay O, Ersoy Z G, Barisci S (2017b). Review—the application of an electro-peroxone process in water and wastewater treatment. Journal of the Electrochemical Society, 164(6): E94–E102

USEIA (2016). Annual Electric Sales, Revenue, and Average Price. Washington: U.S. Energy Information Administration

Valim R B, Reis R M, Castro P S, Lima A S, Rocha R S, Bertotti M, Lanza M R V (2013). Electrogeneration of hydrogen peroxide in gas diffusion electrodes modified with tert-butyl-anthraquinone on carbon black support. Carbon, 61: 236–244

von Gunten U (2018). Oxidation processes in water treatment: are we on track? Environmental Science & Technology, 52(9): 5062–5075

von Sonntag C, von Gunten U (2012). Chemistry of Ozone in Water and Wastewater Treatment: From Basic Principles to Applications. London: IWA Publishing

Wang H, Yuan S, Zhan J, Wang Y, Yu G, Deng S, Huang J, Wang B (2015). Mechanisms of enhanced total organic carbon elimination from oxalic acid solutions by electro-peroxone process. Water Research, 80: 20–29

Wang H, Zhan J, Yao W, Wang B, Deng S, Huang J, Yu G, Wang Y (2018a). Comparison of pharmaceutical abatement in various water matrices by conventional ozonation, peroxone (O_3/H_2O_2), and an electro-peroxone process. Water Research, 130: 127–138

Wang Y, Li X, Zhen L, Zhang H, Zhang Y, Wang C (2012). Electro-Fenton treatment of concentrates generated in nanofiltration of biologically pretreated landfill leachate. Journal of Hazardous Materials, 229–230: 115–121

Wang Y, Yu G, Deng S, Huang J, Wang B (2018b). The electro-peroxone process for the abatement of emerging contaminants: Mechanisms, recent advances, and prospects. Chemosphere, 208: 640–654

Wang Y, Zhou W, Gao J, Ding Y, Kou K (2019). Oxidative modification of graphite felts for efficient H_2O_2 electrogeneration: Enhancement mechanism and long-term stability. Journal of Electroanalytical Chemistry, 833: 258–268

Warsinger D M, Swaminathan J, Guillen-Burrieza E, Arafat H A, Lienhard V J H (2015). Scaling and fouling in membrane distillation for desalination applications: A review. Desalination, 356: 294–313

WHO (2011). Guidelines for Drinking-Water Quality, 4th ed. Geneva: World Health Organization, 324

Xia G, Wang H, Zhan J, Yin X, Wu X, Yu G, Wang Y, Wu M (2020). Evaluation of the stability of polyacrylonitrile-based carbon fiber electrode for hydrogen peroxide production and phenol mineralization during electro-peroxone process. Chemical Engineering Journal, 396: 125291

Xia G, Wang Y, Wang B, Huang J, Deng S, Yu G (2017). The competition between cathodic oxygen and ozone reduction and its role in dictating the reaction mechanisms of an electro-peroxone process. Water Research, 118: 26–38

Yang S, Verdaguer-Casadevall A, Arnarson L, Silvioli L, Čolić V, Frydendal R, Rossmeisl J, Chorkendorff I, Stephens I E L (2018). Toward the decentralized electrochemical production of H_2O_2: A focus on the catalysis. ACS Catalysis, 8(5): 4064–4081

Yao W, Ur Rehman S W, Wang H, Yang H, Yu G, Wang Y (2018). Pilot-scale evaluation of micropollutant abatements by conventional ozonation, UV/O_3, and an electro-peroxone process. Water Research, 138: 106–117

Yu X M, Zhou M H, Ren G B, Ma L (2015). A novel dual gas diffusion electrodes system for efficient hydrogen peroxide generation used in electro-Fenton. Chemical Engineering Journal, 263: 92–100

Yuan S, Li Z X, Wang Y J (2013). Effective degradation of methylene blue by a novel electrochemically driven process. Electrochemistry Communications, 29: 48–51

Zhang H, Chen S, Zhang H G, Fan X F, Cao C, Yu H T, Quan X (2019). Carbon nanotubes-incorporated MIL-88B-Fe as highly efficient Fenton-like catalyst for degradation of organic pollutants. Frontiers of Environmental Science & Engineering, 13(2): 18

Zhang X K, Zhou Y, Zhao C, Sun Z H, Zhang Z G, Mirza Z A, Saylor G, Zhai J, Zheng H L (2016). Electric field induced activated carbon fiber (ACF) cathode transition from an initiator/a promoter into an electrocatalyst in ozonation process. Chemical Engineering Journal, 304: 129–133

Zhou W, Meng X, Gao J, Alshawabkeh A N (2019). Hydrogen peroxide generation from O_2 electroreduction for environmental remediation: A state-of-the-art review. Chemosphere, 225: 588–607